International Conference on Applied Energy 2019
Aug 12-15, 2019, Västerås, Sweden
Paper ID: 0815

FLOW BOILING STABILITY IMPROVEMENT WITH PERIODIC STEPPED FIN MICROCHANNEL HEAT SINK

John Mathew[1], Poh Seng Lee[1*], Tianqing Wu[1], Christopher Yap[1]
1 Department of Mechanical Engineering, National University of Singapore, 9 Engineering Drive 1, Singapore 117575
1* Corresponding Author. Tel.: +65-6516 4187, Email: pohseng@nus.edu.sg

ABSTRACT

A periodic stepped fin microchannel heat sink (PSFMC) is developed to stabilize microchannel flow boiling operation and thereby improve the two-phase heat transfer performance. Flow boiling experiments are performed on the 25mm x 25mm copper based heat sink using de-ionized water as the coolant. The flow boiling performance of this heat sink is benchmarked against a conventional straight microchannel heat sink (SMC).

Unlike the SMC where the confined flow passages lead to bi-directional expansion of elongated vapor slugs, PSFMC facilitates expansion of vapor bubbles or slugs in the span-wise direction at the interconnected sections. Flow reversal effects are minimized and the pressure and temperature measurements are more stable compared to SMC. The improved boiling stability coupled with higher bubble nucleation activity causes the PSFMC to provide an enhanced two-phase heat transfer performance compared to SMC particularly under the lowest mass flux of 57 kg/m^{2}s.

Keywords: microchannel heat sink, two-phase cooling, stability, stepped fin, heat transfer

NONMENCLATURE

Abbreviations

CHF	Critical Heat Flux, W/cm^2
ONB	Onset of Nucleate Boiling
PSFMC	Periodic Stepped Fin Microchannel Heat sink
SMC	Straight Microchannel Heat Sink

Symbols

A	Area, m^2
C_p	Specific heat capacity at constant pressure, J/kgK
d	Distance between wetted wall and nearest thermocouple, mm
G	Mass flux, kg/m^{2}s
H	Height, µm
h	Heat transfer coefficient, W/m^{2}K
I	Current, A
k	Thermal conductivity, W/mK
l	Distance between two rows of thermocouples, mm
$\dot{m}$	Mass flow rate, kg/s
N	Number of channels
N'	Number of interconnected transverse sections
P	Pressure, Pa
ΔP	Pressure drop, Pa
Q	Heating power, W
q''	Heat flux, W/cm^2
T	Temperature, °C
V	Voltage, V
W	Width, µm
z	Streamwise direction
ρ	Density, kg/m^3
η	Fin efficiency
σ	Standard deviation

Subscripts

b	base
c	cross-section
ch	channel
eff	effective
in	heat sink inlet
out	heat sink outlet

r,1	upper thermocouple row
r,2	lower thermocouple row
sat	saturated
tc	thermocouple
w	wall
1	at streamwise position 3mm from the heat sink inlet
2	at streamwise position 7mm from the heat sink inlet
3	at streamwise position 12.5mm from the heat sink inlet
4	at streamwise position 18mm from the heat sink inlet
5	at streamwise position 22mm from the heat sink inlet

1. INTRODUCTION

Two-phase cooling using microchannel heat sinks shows much potential to meet the rising cooling demand of high power density IC devices of the future on account of the much larger heat flux it can dissipate as well as the more uniform device temperature it can maintain compared to single phase liquid cooling. Nevertheless, flow boiling instabilities degrade the heat transfer performance of conventional straight microchannel heat sinks and result in premature CHF.

Although an improved boiling stability is offered by expanding two-phase flow microchannel heat sink configurations such as the diverging microchannels [1], expanding microchannels [2], [3] and stepped fin microchannels [4], they involve the gradual removal of fins in the downstream direction. This leads to a reduction in the convective heat transfer area and also lowers the available bubble nucleation sites [2]. Another approach that has resulted in an improved boiling stability without substantial reduction in wetted area is the use of microchannels with segmented fins where the interconnection of channels provides space for bubbles to expand additionally in the spanwise direction or along secondary channels. In particular, oblique/segmented fin microchannel heat sinks [5], [6] have demonstrated an enhanced heat transfer performance while also stabilizing the flow boiling operation.

Along these lines, a periodic stepped fin microchannel heat sink (PSFMC) is proposed that aims to stabilize boiling operation without substantially removing fins. The design involves partial removal of straight microchannel fins to form 14 interconnected sections that connect the channels in the upper flow region. Such a configuration aims to limit vapor backflow by facilitating spanwise expansion of vapor bubbles/slugs in the interconnected sections.

Flow boiling experiments are carried out using de-ionized (DI) water as the coolant under a range of heat flux and mass flux conditions. The heat transfer performance and boiling stability of this heat sink are compared with its straight microchannel counterpart (SMC). Flow visualization is performed using a high speed camera to study vapor bubble growth behavior and their propagation to the heat sink outlet.

2. EXPERIMENTAL SETUP AND METHODOLOGY

2.1 Experimental setup

The flow loop used for performing the flow boiling experiments is as shown in Fig. 1. The coolant, DI water, is circulated through the flow loop using a gear pump following a degassing procedure. DI water is pumped to the test section where it is maintained at a constant temperature of 85.5°C at the inlet. Upon exiting the test section, the water is cooled back to ambient conditions in an air cooled condenser after which it returns to the reservoir.

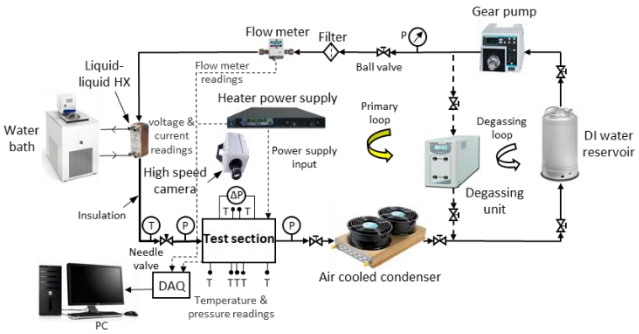

Fig 1 Schematic of experimental flow loop

The test section comprises of an acrylic top cover, a top housing made of PEEK (polyetheretherketone), the copper heat sink assembly, and a bottom housing made of PTFE. Fig. 2 provides a schematic of the individual test section components. Two T-Type thermocouples (dia. 1/16", Omega) are used to measure the coolant temperatures at the inlet and outlet while ten other T-Type thermocouples (dia. 0.5mm, Omega) obtain temperature measurements of the heat sink at different locations. Pressure drop across the heat sink is measured using a differential pressure transducer (Omega PX409 G2.5DWU10V). A high speed camera (Photron FASTCAM SA5 1000K-M3) is used to perform flow visualization.

The PSFMC heat sink is made of copper and has a 25mm x 25mm footprint. It consists of 40 straight

microchannels with nominal cross-section of 300µm (W_{mc}) x 600µm (H_{mc}). Sections of the straight fins are reduced to half the channel height at various locations along the streamwise direction. This leads to the formation of 14 interconnected transverse sections, each having a width of 23.7mm and depth of 300µm. The resultant fins have a periodic stepped profile with full fins being 1200µm in length while the half fin steps being 500µm in length. Fig. 3 describes the PSFMC design, more specifically called PSFMC 14-0.5. The straight microchannel (SMC) counterpart of this heat sink has 40 channels with nominal cross-section of 300µm (W_{mc}) x 600µm (H_{mc}).

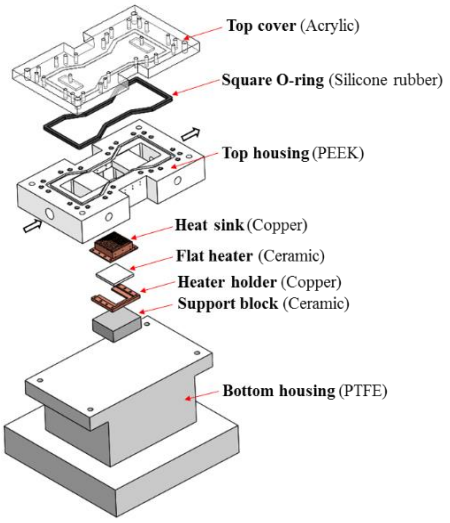

Fig 2 Schematic image of test section components

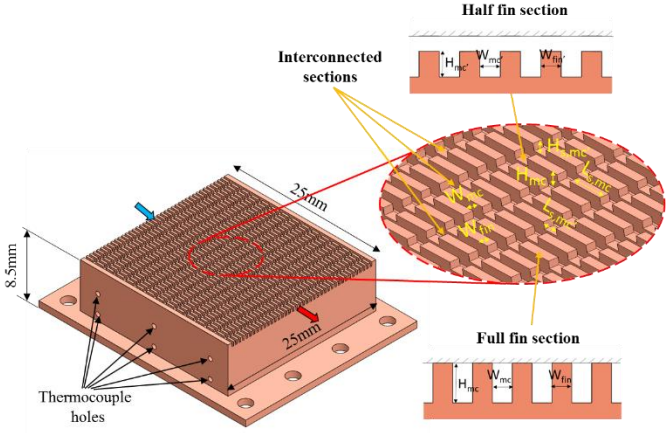

Fig 3 Schematic image describing geometrical design of PSFMC 14-0.5 heat sink

2.2 Experimental procedure

Both the PSFMC and SMC are tested under mass fluxes of 57 kg/m^{2}s, 113 kg/m^{2}s and 227 kg/m^{2}s. The heat flux is incremented from 0-140 W/cm^2. Steady state conditions are reached in 15-20 min for each heat input condition when temperature readings fluctuate under ±0.5°C over 2-3 min. The measurement data from the flow meter, pressure transducers, thermocouples and power supply unit are recorded at 50Hz over a period of 120s by a data acquisition system (NI cDAQ-9172).

2.3 Data reduction and uncertainty analysis

The effective heat power supply to the copper block is obtained by deducting the heat loss, Q_{loss}, from the heating power supply as,

$$Q_{eff} = Q_{supply} - Q_{loss} \quad (1)$$

With respect to the base area of the heat sink, A_b = W_b x L_b, the effective heat flux is calculated as,

$$q"_{eff} = \frac{Q_{eff}}{A_b} \quad (2)$$

The heat flux between the two rows of thermocouples, at each streamwise thermocouple location, z, is determined based on the 1-D conduction assumption as,

$$q"_{z,tc} = k_{Cu}\frac{(T_{z,tc,r2} - T_{z,tc,r1})}{l} \quad (3)$$

Where l is 3mm. Now, the local wall temperature is obtained by considering 1-D heat conduction between the upper thermocouple and the base wetted area of the heat sink,

$$T_{w,z} = T_{z,tc,r1} - \frac{q"_{z,tc}d}{k_{Cu}} \quad (4)$$

where d is 2.9mm. It should be noted that the two-phase heat transfer performance is compared based on the most downstream thermocouple position, z_5, where the boiling intensity is greatest.

Under saturated boiling conditions, the local fluid temperature at z_5 is set to the saturation temperature corresponding to the outlet pressure such that,

$$T_{f,z5} = T_{sat,P_{out}} \quad (5)$$

Uncertainty analysis of the derived variables is performed using the error estimation method provided by Taylor [7]. A maximum error of ± 0.27% is associated with the effective heat flux while that of the heat transfer coefficient ranges between 8-15%.

3. EXPERIMENTAL RESULTS AND DISCUSSIONS

3.1 Boiling curves

Fig. 4 (a)-(c) shows the flow boiling curves of PSFMC and SMC under mass fluxes of 57 kg/m^{2}s, 113 kg/m^{2}s and 227 kg/m^{2}s respectively. It can be seen that PSFMC is able to maintain a lower wall superheat than SMC for a given heat flux across the entire range of operating heat flux. This lowering of wall temperature with PSFMC

becomes more pronounced with reducing mass flux. At the lowest mass flux of G = 57 kg/m^{2}s, it can be observed in Fig. 4 (a) that the performance of SMC degrades at an effective heat flux of 89 W/cm^2 and consequently reaches CHF earlier. Whereas, PSFMC is able to operate upto the highest heat flux without experiencing CHF. This is due to the improved boiling stability associated with PSFMC as will be explained later. During the experiments, CHF is identifed as the effective heat flux for which the wall temperature rises rapidly without reaching steady state.

A similar trend in boiling curves can be seen at the moderate mass flux of G = 113 kg/m^{2}s where SMC experiences CHF at an effective heat flux of 136.9W/cm^2 while PSFMC maintains a lower wall temperature and delays CHF. However, as mass flux increases, the performance of SMC improves and its boiling curves can be seen to approach that of PSFMC. At the highest mass flux of G = 227 kg/m^{2}s, it can be seen from Fig. 4 (c) that the wall superheat of SMC at the highest heat flux is 8.2°C while the corresponding wall superheat for PSFMC

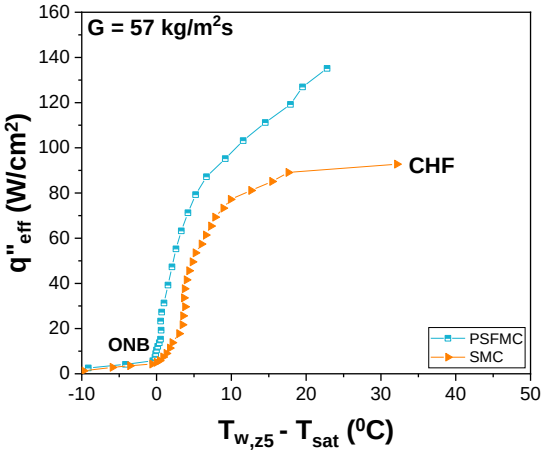

(a)

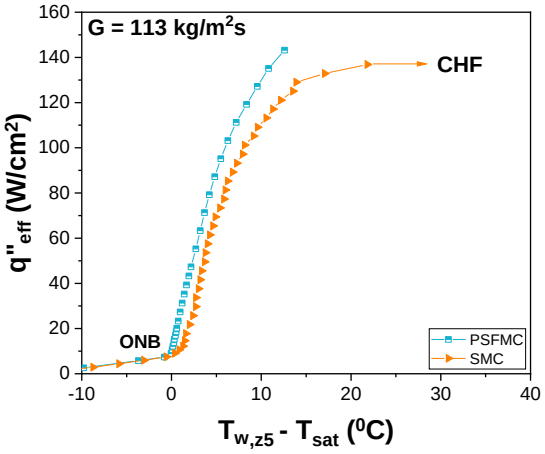

(b)

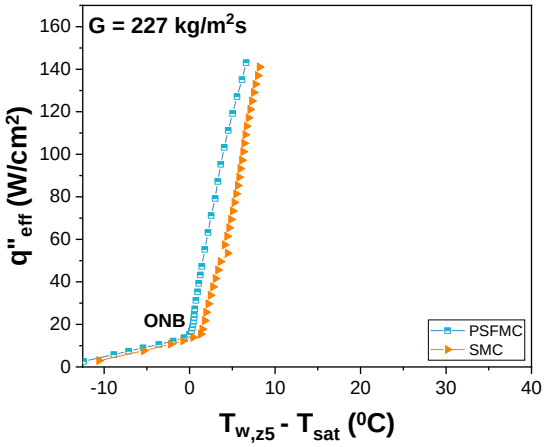

(c)

Fig 4 Boiling curves of PSFMC and SMC under mass fluxes of (a) G = 57 kg/m^{2}s, (b) G = 113 kg/m^{2}s and (c) G = 227 kg/m^{2}s

is 6.7°C. The difference in wall superheat is lesser than that at lower mass fluxes. Maximum wall superheat reductions of 10.9°C, 6.3°C and 2.3°C are attained by PSFMC at mass fluxes of 57 kg/m^{2}s, 113 kg/m^{2}s and 227 kg/m^{2}s respectively.

From the boiling curves presented in Fig. 4, it can be observed that ONB in PSFMC occurs at a lower wall superheat than SMC, particularly for the mass flux cases of 113 kg/m^{2}s and 227 kg/m^{2}s as shown in Fig. 4 (b) and (c) respectively. The presence of the large number of edges and corners associated with the multiple stepped fin sections in PSFMC leads to a greater number of bubble nucleation sites compared to SMC [5], [6], [8]. This is evident from the flow visualization images shown in Fig. 5 (a) and (b) that compare the bubble nucleation density of PSFMC with that of SMC under similar operating conditions.

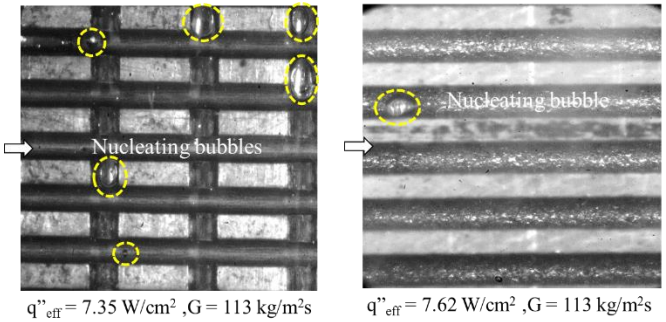

(a) (b)

Fig 5 Flow visualization images comparing bubble nucleation density of (a) PSFMC and (b) SMC at mass flux of 113 kg/m^{2}s

At high heat flux, an annular flow regime is established in both PSFMC and SMC. The flow pattern consists of the passage of a vapor core through the channel surrounded by a thin liquid film on the channel walls. Thin film evaporation is the two-phase heat transfer mechanism during this regime [4], [9], [10]. In the case of PSFMC, the repeated interruptions at the multiple interconnected sections cause the annular flow in the channels to get disrupted. This phenomenon is demonstrated in Fig. 6. Such an interrupted annular flow does not take place in SMC. In addition, the wake zones at the trailing faces of each step in PSFMC are poorly wetted as annular flow gets disrupted upon expansion at each interconnected section. Due to these effects, the thin film evaporation mechanism is not as effective as in SMC.

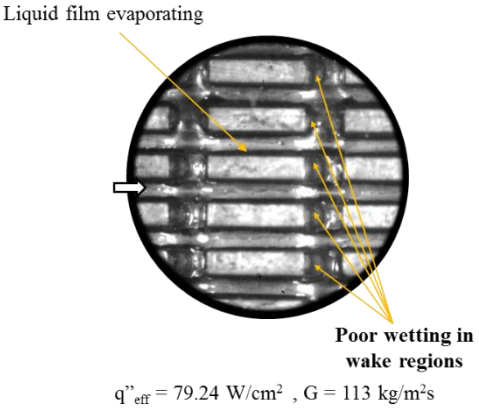

Fig 6 Flow visualization image of PSFMC demonstrating interrupted annular flow with dry-out regions on the stepped fin faces located in the trailing regions of the full fins

This explains the increasing wall superheat of PSFMC at high heat flux under the low and moderate mass flux conditions of 57 kg/m^{2}s and 113 kg/m^{2}s respectively as observed in Fig. 4 (a) and (b). In the case of SMC, the annular flow regime established at moderate to high heat flux does not undergo such interruptions. Consequently, it provides a more effective thin film evaporation mechanism.

The other reason for the enhancement in PSFMC heat transfer performance and elevated CHF, particularly at 57 kg/m^{2}s and 113 kg/m^{2}s, is the more stable boiling operation it offers compared to SMC. Unlike the case of SMC where vapor bubbles/slugs are forced to expand in the forward and reverse directions, vapor bubbles/slugs in PSFMC primarily expand in the spanwise direction in one of the 14 interconnected sections that link the upper half regions of the channel flow. As vapor expansion is predominantly in the transverse direction, flow reversal effects are minimized. Fig. 7 (a) demonstrates spanwise vapor slug expansion that results in negligible backflow compared to Fig. 7 (b) which shows the rapid streamwise vapor slug expansion taking place in SMC.

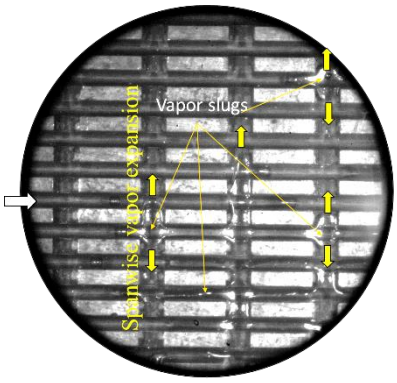

(a)

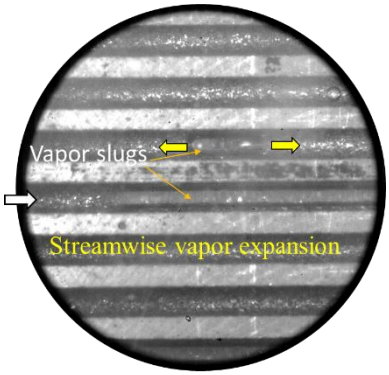

(b)

Fig 7 Flow visualization images showing vapor expansion behavior in (a) PSFMC and (b) SMC at G = 113 kg/m2s

3.2 Flow boiling stability

The improved boiling stability of PSFMC is also indicated by the reduced fluctuations in pressure drop measurements of PSFMC compared to SMC. Fig. 8 (a)-(b) shows the standard deviation of pressure drop fluctuations over 120s as a function of effective heat flux for PSFMC and SMC under mass fluxes of 57 kg/m^{2}s and 227 kg/m^{2}s respectively. A lower standard deviation in pressure drop fluctuations indicates an improved boiling stability with lesser flow oscillations. At the lowest mass flux of 57 kg/m^{2}s, it can be inferred from Fig. 8 (a) that the flow oscillations in PSFMC are much lower than SMC. The greater degree of flow reversal effects in SMC results in a degradation of heat transfer performance with increasing heat flux. This becomes more pronounced at lower mass fluxes where SMC experiences severe partial dry-out followed by CHF at comparatively lower heat fluxes.

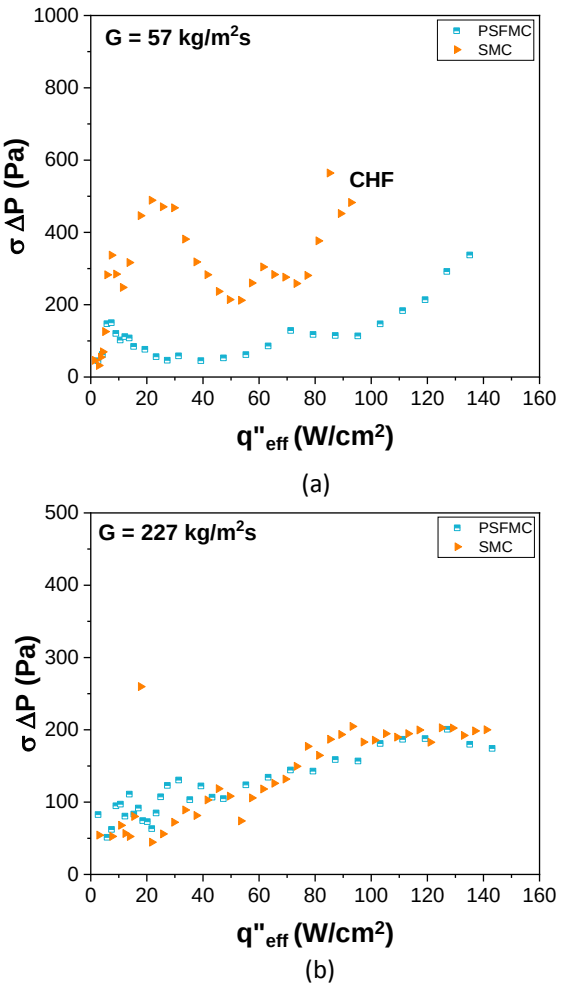

Fig 8 Comparison of flow boiling stability of PSFMC and SMC in terms of standard deviation of pressure drop fluctuations at (a) lowest mass flux of 57 kg/m^{2}s and (b) highest mass flux of 227 kg/m^{2}s

However, with increasing mass flux, the boiling stability of PSFMC becomes less pronounced when compared to SMC as seen in Fig. 8 (b).

4. CONCLUSIONS

A periodic stepped fin microchannel heat sink (PSFMC) is developed to stabilize flow boiling operation. Compared to its straight microchannel heat sink counterpart (SMC), PSFMC outperforms across the whole range of operating heat flux at the lowest mass flux of 57 kg/m^{2}s. Whereas, it offers an enhanced performance only over the range of low to moderate heat flux under the moderate and high mass flux conditions of 113 kg/m^{2}s and 227 kg/m^{2}s respectively. The augmented heat transfer performance of PSFMC is attributed to the improved boiling stability and increased bubble nucleation density compared to SMC. The improved boiling stability in PSFMC is due to the spanwise expansion of vapor slugs at the interconnected sections that limits vapor backflow. As a result, CHF is delayed in PSFMC unlike SMC.

ACKNOWLEDGEMENT

The authors gratefully acknowledge the funding from Infocomm Media Development Authority (IMD, Singapore (WBS No. R265-000-574-490) that supported this work.

REFERENCE

[1] C. T. Lu and C. Pan, “Stabilization of flow boiling in microchannel heat sinks with a diverging cross-section design,” J. Micromechanics Microengineering, vol. 18, no. 7, p. 075035, 2008.

[2] K. Balasubramanian, P. S. Lee, L. W. Jin, S. K. Chou, C. J. Teo, and S. Gao, “Experimental investigations of flow boiling heat transfer and pressure drop in straight and expanding microchannels - A comparative study,” Int. J. Therm. Sci., vol. 50, no. 12, pp. 2413–2421, 2011.

[3] H. J. Lee and S. chune Yao, “System instability of evaporative micro-channels,” Int. J. Heat Mass Transf., vol. 53, no. 9–10, pp. 1731–1739, 2010.

[4] K. Balasubramanian, P. S. Lee, C. J. Teo, and S. K. Chou, “Flow boiling heat transfer and pressure drop in stepped fin microchannels,” Int. J. Heat Mass Transf., vol. 67, pp. 234–252, 2013.

[5] M. Law and P. S. Lee, “A comparative study of experimental flow boiling heat transfer and pressure characteristics in straight- and oblique-finned microchannels,” Int. J. Heat Mass Transf., vol. 85, pp. 797–810, 2015.

[6] Y. K. Prajapati, M. Pathak, and M. Kaleem Khan, “A comparative study of flow boiling heat transfer in three different configurations of microchannels,” Int. J. Heat Mass Transf., vol. 85, pp. 711–722, 2015.

[7] J. Taylor, “Introduction to Error Analysis, the Study of Uncertainties in Physical Measurements, 2nd Edition,” Published by University Science Books. p. 327, 1997.

[8] S. G. Kandlikar, W. K. Kuan, D. A. Willistein, and J. Borrelli, “Stabilization of Flow Boiling in Microchannels Using Pressure Drop Elements and Fabricated Nucleation Sites,” J. Heat Transfer, vol. 128, no. 4, p. 389, 2006.

[9] W. Qu and I. Mudawar, “Measurement and correlation of critical heat flux in two-phase micro-channel heat sinks,” Int. J. Heat Mass Transf., vol. 47, no. 10–11, pp. 2045–2059, 2004.

[10] A. Tamanna and P. S. Lee, “Flow boiling heat transfer and pressure drop characteristics in expanding silicon microgap heat sink,” Int. J. Heat Mass Transf., vol. 82, no. November, pp. 1–15, 2015.